METTL3-mediated m6A methylation negatively modulates autophagy to support blastocyst development

Zubing Cao
Anhui Agricultural University
Ling Zhang
Anhui Agricultural University
Renyun Hong
Anhui Agricultural University
Yiqing Wang
Anhui Agricultural University
Xin Qi
Anhui Agricultural University
Wei Ning
Anhui Agricultural University
Di Gao
Anhui Agricultural University
Tengteng Xu
Anhui Agricultural University
Yangyang Ma
Anhui Agricultural University
Tong Yu
Anhui Agricultural University
Yunsheng Li
Anhui Agricultural University
Jason G Knott
Michigan State University
Anucha Sathanawongs
Chiang Mai University
Yunhai Zhang (yunhaizhang@ahau.edu.cn)
Anhui Agricultural University https://orcid.org/0000-0001-9721-5910

Research

Keywords: METTL3, m6A methylation, Blastocyst, ATG5, Autophagy

Posted Date: May 11th, 2020

DOI: https://doi.org/10.21203/rs.3.rs-27238/v1

Abstract

Background: N^6-methyladenosine (m6A) catalyzed by METTL3 regulates the maternal-to-zygotic transition in zebrafish and mice. However, the role and mechanism of METTL3-mediated m6A methylation in blastocyst development remains unclear.

Results: We found that reduced m6A levels triggered by *METTL3* knockdown caused embryonic arrest during morula-blastocyst transition and developmental defects in trophectoderm cells. Intriguingly, overexpression of *METTL3* in early embryos resulted in increased m6A levels and these embryos phenocopied *METTL3* knockdown embryos. Mechanistically, *METTL3* knockdown or overexpression resulted in a significant increase or decrease in expression of ATG5 and LC3 (an autophagy marker) in blastocysts, respectively. m6A modification of ATG5 mRNA mainly occurs at 3'UTR, and *METTL3* knockdown enhanced *ATG5* mRNA stability, suggesting that METTL3 negatively regulated autophagy in an m6A dependent manner. Furthermore, single-cell analysis revealed that *METTL3* knockdown only increased expression of LC3 and *ATG5* in trophectoderm cells, indicating preferential inhibitory effects of METTL3 on autophagy activity in the trophectoderm lineage. Importantly, autophagy restoration by 3MA (an autophagy inhibitor) treatment partially rescued developmental defects of *METTL3* knockdown blastocysts.

Conclusions: Our results demonstrate that METTL3-mediated m6A methylation negatively modulates autophagy to support blastocyst development.

Introduction

Mammalian blastocyst formation is accompanied with the formation of trophectoderm (TE) and inner cell mass (ICM) lineages[1–3]. Establishment of the functional TE lineage is an essential prerequisite for blastocyst and placenta development. TE cells require a larger amount of ATP than ICM cells to form and expand the blastocoel cavity [4, 5]. Aberrant energy metabolism in TE cells is closely related to the impaired TE lineage specification and blastocyst development [6]. Thus, understanding metabolic regulatory mechanisms underlying TE cell formation is a fundamental question in mammalian blastocyst development.

Autophagy is an essential catabolic process that degrades cellular proteins and organelles into simple molecules to generate nascent energy. Autophagy process is negatively regulated by mTOR (mammalian target of rapamycin) and positively controlled through a set of autophagy-related (ATG) genes [7]. Although physiological levels of autophagy are required for mammalian early embryo development [8], excessive levels of autophagy frequently impair cell viability [9]. For instance, *ATG5*-deleted mouse embryos arrested at the 4-cell stage [10]. Reduced levels of autophagy prevented porcine blastocyst formation [11, 12]. It was worth noting that autophagy activity was preferentially restricted to TE cells relative to ICM cells in mouse blastocysts [13]. Remarkably, autophagy induction by the inhibition of mTOR restored energy metabolism of *TEAD4*-deficient TE cells to allow TE lineage specification and

blastocyst development [4]. To date, despite our current knowledge on the epigenetic mechanisms that modulate autophagy at the DNA and histone levels [14], little has been known about the fine-tuning mechanism of autophagy through post-transcriptional RNA modification.

N^6-methyladenosine (m6A), the most abundant internal modification on eukaryotic message RNAs (mRNAs), happens extensively at 5'untranslated region (5'UTR), coding sequence (CDS), and 3'UTR [15]. Recent studies showed that m6A methylation is a reversible dynamic modification that is mainly written by the core enzyme methyltransferase-like protein 3 (METTL3) and erased by the demethylase fat mass and obesity-associated protein (FTO) [16]. The m6A modification has been demonstrated at the molecular levels to regulate RNA stability, decay, translation, alternative splicing, and exportation [17]. It was recently reported that m6A methylation participated in controlling animal reproduction-associated developmental events, such as spermatogenesis [18, 19], oogenesis [20], gamete maturation [21–23], oocyte-to-embryo transition [20, 24], and blastocyst formation [25]. However, the underlying mechanism on the role of m6A in blastocyst development remains unclear. Of note, the phenomena of m6A modification negatively correlating with autophagy activity have been clearly documented in several different cellular contexts [26–28]. We thus hypothesized that METTL3-mediated m6A methylation might regulate blastocyst development via repressing autophagy activity.

In the present study, porcine embryos were used as a model to test this hypothesis. We showed that METTL3 negatively regulates expression of *ATG5* mRNA in an m6A-dependent manner, thereby repressing autophagy activity to sustain porcine blastocyst development. Moreover, lineage-specific analyses indicated that m6A modification preferentially inhibits autophagy activity in the trophectoderm lineage. These findings provide new insights into the post-transcriptional epigenetic regulation of blastocyst development.

Methods

Oocyte maturation

Porcine ovaries were collected from a local slaughterhouse. Follicular fluid was aspirated from antral follicles at 3–6 mm in diameter. Cumulus-oocyte complexes (COCs) were selected under a stereomicroscope. Subsequently, COCs were cultured in a 4-well plate containing 400 μL *in vitro* maturation medium (TCM-199 supplemented with 5% FBS, 10% porcine follicular fluid, 10 IU/mL eCG, 5 IU/mL hCG, 100 ng/mL L-Cysteine, 10 ng/mL EGF, 0.23 ng/mL melatonin, 2.03×10^{-5} ng/mL LIF, 2×10^{-5} ng/mL IGF-1, 4×10^{-5} ng/mL FGF2, 100 U/mL penicillin and 100 mg/mL streptomycin) for 44 h at 38.5 ºC, 5% CO_2 and saturated humidity. Cumulus cells surrounding oocytes was removed using 1 mg/mL hyaluronidase following maturation.

Parthenogenetic activation (PA)

MII (metaphase II) oocytes were stimulated using two pulses of direct current (1.56 kV/cm for 80 ms) in activation medium (0.3 M mannitol supplemented with 0.1 mM $CaCl_2$, 0.1 mM $MgCl_2$ and 0.01% polyvinyl

alcohol). Subsequently, activated oocytes were washed with porcine zygote medium (PZM-3) three times and were incubated in the chemically assisted activation medium (PZM-3 supplemented with 10 μg/mL cycloheximide and 10 μg/mL cytochalasin B) for 4 h. Then, embryos were cultured in PZM-3 droplets at 38.5 °C, 5% CO_2 and 95% air with saturated humidity.

In vitro fertilization (IVF)

MII oocytes were washed in the modified Tris-buffered medium (mTBM) containing 2 mg/mL BSA and 2 mM caffeine. Approximately 15 oocytes were incubated in 50 μL droplets of mTBM for 4 h at 38.5 °C in 5% CO_2 in air. Semen from two boars was mixed and centrifuged at 1900 g for 4 min in DPBS supplemented with 1 mg/mL BSA (pH 7.3). Then, sperm was resuspended with mTBM to a concentration of 1×10^6 cells/mL. Fifty microliters of sperm solution were added to the mTBM droplets containing oocytes. After co-incubation of oocytes and sperm for 6 h, excess sperm surrounding oocytes were washed out and presumptive zygotes were cultured in PZM-3 at 38.5 C in 5% CO_2 in air.

In vitro transcription

METTL3-EGFP mRNA used for microinjection was synthesized in vitro. pIVT- METTL3-EGFP plasmid containing T7 promoter was linearized by digestion with BspQI. Linearized DNA templates were purified using a DNA clean & concentrator Kit (ZYMO RESEARCH, D4003, Tustin, CA, USA). According to the manufacture's manual, *in vitro* transcription of *METTL3-EGFP* mRNA was performed through using mMESSAGE MACHINE TM T7 kit (Ambion, AM1344, shanghai, China) and Poly (A) Tailing Kit (Ambion, AM1350, Shanghai, China). Then, mRNA was treated with TURBO Dnase to remove the DNA templates and was further purified using MEGAclear Kit (Ambion, AM1908, Shanghai, China). After dissolving mRNA in RNase-free water, mRNA concentration was determined by a Nanodrop instrument (Thermo Scientific, Shanghai, China) and was then aliquoted and stored at -80 °C.

Microinjection

siRNA species were designed to target three different sites of the porcine *METTL3* coding region (GenePharma, Shanghai, China). Information on the siRNA sequences used in this study was listed in Table 1. Microinjection was performed in a T2 (TCM199 with 2% FBS) medium containing 7.5 μg/ml Cytochalasin B on an inverted microscope (Olympus, Japan). Approximately 10 pl of siRNA solution (50 μM) was microinjected into the cytoplasm of MII oocytes. Embryos were cultured in PZM-3 medium for 7 days.

Table 1
Information on METTL3 siRNA sequences

No. siRNA	Sequence (5'-3')	
	Sense	Antisense
1	GCACUCGAAAGAUUGAAUUTT	AAUUCAAUCUUUCGAGUGCTT
2	GCAUUGGAUCUUCGGAAUTT	AUUCCGAAGAUCCAAGUGCTT
3	GCAAGAAUUCUGUGACUAUTT	AUAGUCACAGAAUUCUUGCTT

Real-time quantitative PCR (qPCR)

Total RNA was extracted from oocytes and embryos using RNeasy Mini Kit (Qiagen, 74104). RNA was transcriptionally reversed into cDNA using QuantiTect Reverse Transcription Kit (Qiagen, 205311). cDNA was aliquoted and was stored at -80 ºC. The primers used in this study were listed in Table 2. The assembly of polymerase chain reaction was prepared in FastStart SYBR Green Master (Roche, 04673514001) and was run on StepOne Plus (Applied Biosystems, Foster, USA). The samples were collected three times and three biological replicates were conducted for each gene. *EF1A1* was used as the internal reference gene. The Cq values were obtained and analyzed using the $2^{-\Delta\Delta Ct}$ method.

Table 2
Porcine-specific primer sequences used in this study

Gene symbol	Primer sequences (5'-3')	Product size (bp)	GenBank accession number
METTL3	F: CTGGGGTTACGAACGGGTAG	125	XM_003128580.5
	R: TGACACCAACCAAGCAGTGT		
METTL14	F: GGGAGAGTGTGTTTACGCAAGTG	145	XM_003129231.6
	R: TTCCCATAAGGCAGTGTTCCTT		
WTAP	F: CTGCACGCAGGGAAAACAT	140	XM_005659114.3
	R: TGGGTCGACCATTGTTGATCT		
ATG5	F: GGTTTGAATATGAAGGCACACCA	100	NM_001037152.2
	R: TGTGATGTTCCAAGGAAGAGCTG		
BECLIN1	F: AGGAGCTGCCGTTGTACTGTTCT	105	NM_001044530.1
	R: TGCTGCACACAGTCCAGGAA		
LC3	F: AACGAAATTCCTGGTGCCTGA	101	NM_001170827.1
	R: AAGGCTTGGTTAGCATTGAGCTG		
BCL2	F: GGTACCGGAGGGCATTCAGT	100	NM_214285
	R: TCCCGGAAGAGTTCGTTCAC		
BAX	F: TGCTTCAGGGTTTCATCC	112	XM_003127290.4
	R: AGACACTCGCTCAACTTC		
CASPASE3	F: GGATTGAGACGGACAGTG	109	NM_214131.1
	R: CGCCAGGAATAGTAACCAG		
P53	F: CCACCATCCACTACAACTTC	135	NM_213824.3
	R: AAACACGCACCTCAAAGC		
SOX2	F: CGCAGACCTACATGAACG	103	NM_001123197.1
	R: TCGGACTTGACCACTGAG		
CDX2	F: AGTCGCTACATCACCATTCGGAG	139	NM_001278769.1

Gene symbol	Primer sequences (5'-3')	Product size (bp)	GenBank accession number
	R: GCTGCTGTTGCTGCAACTTCTTC		
EF1a1	F: ATTGTTGCTGCTGGTGTTG	161	NM_001097418-2
	R: TCATATCTCTTCTGGCTGTAGG		
F: forward, R: reverse			

Single-cell qPCR

Primer pool containing multiple genes was prepared according to the instructions of the Single Cell Sequence Specific Amplification Kit (Vazyme, P621-01, Nanjing, China). Individual blastomeres or embryos were transferred into Master Mix and immediately transcriptionally reversed into cDNA at -80 ºC for 2 min. Then, the amplification of cDNA was performed according to the manufacture's manual. The relative levels of the target genes were detected on a StepOne Plus real-time PCR system (Applied Biossystems) using a pre-amplified cDNA as a template using SYBR Green PCR Master Mix (Applied Biossystems).

Identification of TE and ICM blastomeres of blastocysts

Zona pellucida of blastocysts was removed by digestion of 3.3 mg/mL pronase for 3 min. Zona-free blastocysts were incubated in 0.25% trypsin for 40 min. Individual blastomeres were isolated by repeated pipetting of blastocysts with glass needle at 100 μm in diameter. Individual blastomeres were lysed using single cell quantitative kit. Samples were pre-amplified for 20 cycles according to the manufacture's protocol. The relative levels of *SOX2* and *CDX2* mRNA were detected by single-cell qPCR. Then, data were further analyzed by principal component analysis (PCA) using SIMCA14.1 software [29]. Blastomeres from TE and ICM were identified according to the clustering analyses.

mRNA stability

Embryos at the morula stage were treated with 25 μg/mL α-amanitin (MCE, HY-19160) to inhibit global mRNA transcription. Embryos were collected at 0, 12, 24, 36, 48, and 60 h and total RNA was extracted for reverse transcription. The levels of *ATG5* mRNA were determined using single-cell qPCR.

Immunofluorescence staining

Oocytes and embryos were fixed in 4% paraformaldehyde solution for 15 min, permeabilized with 1% Triton X-100 for 30 min at room temperature (RT) and then blocked with 2% BSA at RT for 1 h. Samples were incubated in solution containing primary antibodies overnight at 4 °C. After washing, samples were incubated for 1 h in solution containing secondary antibodies in the dark at 37 °C. Afterwards, samples were counterstained using 4, 6-diamidino-2-phenylindole dihydrochloride or propidium iodide for 10 min and were then loaded onto glass slides. Finally, samples were imaged using laser scanning confocal

microscopy (Olympus, Japan). The average pixel intensity of embryos was determined using Image J. Information regarding primary and secondary antibodies used was listed in Table 3.

Table 3
Information on antibodies used in the present study

Primary Antibody	**Species**	**Vendor**	**Cat.no.and dilution**
m6A	Rabbit	abcam	ab190866 (1:75)
CDX2	Mouse	Biogenex	AM392 (ready to use)
ATG5	Rabbit	Bioss	bs-4005R(1:200)
LC3B	Rabbit	Cell Signaling	2775S (1:200)
Secondary Antibody	**Species**	**Vendor**	**Cat.no.and dilution**
Alexa Fluor 488 anti-mouse IgG	Goat	Invitrogen	A11029 (1:200)
Alexa Fluor 594 anti-mouse IgG	Goat	Invitrogen	A11005 (1:200)
Alexa Fluor 488 anti-rabbit IgG	Goat	Invitrogen	A11008 (1:200)
Alexa Fluor 594 anti-rabbit IgG	Goat	Invitrogen	A11012 (1:200)

Treatment of embryos with 3MA

The 3-methyladenine autophagy inhibitor, 3MA (MCE, HY-19312) was dissolved in PZM-3 and stored at -20 °C until it was used. Working solution of 0.1 mM 3MA was prepared in PZM-3. To evaluate the effects of 3MA on autophagy and blastocyst development, morula was cultured in the presence and absence of 3MA for 72 h.

TdT (terminal deoxynucleotidyl transferase)-mediated dUDP nick-end (TUNEL) staining

Blastocysts were fixed in 4% PFA for 15 min at RT. Following several washing, blastocysts were incubated in DNase I (TIANGEN, RT411, China) for 1 h at 38.5 °C. After washing, blastocysts with the treatment of label solution (In Situ Cell Death Detection Kit, 7791-13-1, Roche, Germany) served as the negative control group. Blastocysts with the treatment of enzyme solution served as the positive control group. Blastocysts without the treatment of DNase I from other groups were directly incubated in enzyme solution for 1 h. All blastocysts were stained with DAPI for 15 min and were then imaged using laser scanning confocal microscopy (Olympus, Japan). Total number of cells and number of apoptotic dead cells were counted and apoptotic ratio were calculated by dividing the number of dead cells by the total number of cells, which included dead cells.

Statistical analysis

All experiments were carried out at least three times. Data were analyzed using one-way ANOVA or student's *t* test (SPSS 17.0) and were presented as mean ± standard error of mean (mean ± S.E.M). $P <$

0.05 was considered to be statistically significant.

Results

Characterization of m6A methylation and its writers in early embryos

To investigate the kinetics and subcellular localization of m6A methylation in early embryos, immunofluorescence staining was performed to characterize dynamic patterns of m6A modification. The specificity of commercially available m6A antibody in porcine embryos had been verified by RNase A treatment (Additional file 1a and b). The results in PA embryos revealed that m6A levels in oocytes and blastocysts appeared to be higher than that in embryos from 2-cell to morula stage, and m6A methylation occurred in cytoplasm from GV oocyte to morula stage whereas m6A modification are present in nucleus and cytoplasm of blastocysts (Fig. 1a). Similarly, the highly dynamic patterns and localization of m6A modification were also observed in IVF embryos (Fig. 1b). To determine whether transcripts encoding m6A writers including *METTL3*, *METTL14* and *WTAP* are expressed in early embryos, qPCR was performed to examine its relative abundance. We found a persistent expression of the three genes during meiotic maturation and subsequent early embryo development, suggesting its maternal and zygotic origins (Fig. 1c, d and e). However, the expression levels of genes were a little lower through morula to blastocyst stage relative to oocytes and early-cleavage embryos (Fig. 1c, d and e) ($P < 0.05$). Therefore, these results indicate m6A modification and its writers are dynamically present in early embryo development.

METTL3 knockdown impedes blastocyst development and trophectoderm lineage formation

To explore the biological role of endogenous METTL3 in early embryo development, siRNAs against *METTL3* were microinjected into MII oocytes. Meanwhile, noninjected and negative control (NC) siRNA-injected MII oocytes served as control groups. qPCR results showed that *METTL3* siRNA injection significantly reduced the levels of *METTL3* mRNA at the 4-cell stage compared to the control groups (Fig. 2a) ($P < 0.05$). Unfortunately, we did not directly analyze the influence of METTL3 siRNA injection on METTL3 protein levels because of the lack of porcine specific METTL3 antibodies. Alternatively, *METTL3-EGFP* mRNA and siRNA were coinjected into oocytes served as experimental group, noninjected, *EGFP* mRNA or *METTL3* siRNA injection alone served as control groups. Fluorescence intensity analyses revealed that *METTL3* siRNA injection significantly reduced the levels of METLL3 protein at the 4-cell stage compare to the control groups (Fig. 2b)($P < 0.05$). Furthermore, a subset of embryos at 2-cell, 4-cell and blastocyst stage were isolated and subjected to immunofluorescence staining to detect m6A levels. *METTL3* siRNA injection significantly reduced m6A levels at the aforementioned stages compared to the

control groups (Fig. 2c, d and e)($P < 0.05$). Of note, no differences in the levels of *METTL3* mRNA, protein and m6A were observed between the NC siRNA injected and uninjected control groups.

To determine whether *METTL3* knockdown (referred to as *METTL3* KD) affected early embryo development, the developmental rates of *METTL3* KD embryos were compared to NC siRNA and uninjected embryos. We found that *METLL3* KD had no influence on development to 2-cell, 4-cell, 8-cell and morula stage (additional file 2), but compromised the development to blastocyst stage (Day 5–7) compared to the control groups (Fig. 2f and g)($P < 0.05$). A small proportion of *METTL3* KD embryos developed to the blastocyst stage (Fig. 2f), we then analyzed the lineage allocation in these blastocysts. Blastocysts were stained with a CDX2 antibody to label the TE cells (Fig. 2h). The number of inner cell mass (ICM) cells was indirectly determined by subtracting the TE number from the total cell number. The results revealed that ICM cell number did not change between *METTL3* KD and the control groups (Fig. 2i). However, *METTL3* KD resulted in a significant reduction in both total cell number and TE cell number (Fig. 2i) ($P < 0.05$). Additionally, the ratio of ICM cells to TE cells in the *METTL3* KD blastocysts significantly increased compared to the control groups (Fig. 2i) ($P < 0.05$). Therefore, these data demonstrate that METTL3 is required for porcine blastocyst development and TE lineage formation.

METTL3 negatively regulates blastocyst development and perturbs normal lineage allocation

We next investigated whether overexpression of *METTL3* could affect embryonic development. *METTL3-EGFP* mRNA was introduced into the cytoplasm of MII oocytes. Uninjected and *EGFP* mRNA-injected MII oocytes served as control groups. qPCR and fluorescence intensity analyses were performed to determine the relative expression of *METTL3* mRNA and protein in the subset of embryos at the 2-cell, 4-cell and blastocyst stage. The results showed that *METLL3-EGFP* mRNA injection indeed induced a higher expression of *METTL3* mRNA (Fig. 3a, b and c) and protein (Fig. 3d, e and f) at the aforementioned stages compared to the control groups ($P < 0.05$). To determine the effect of *METTL3* overexpression (referred to as *METTL3* OE) on early embryo development, the developmental rates of embryos were analyzed. Unexpectedly, *METTL3* OE did not affect the development rate of 2-cell embryos (Fig. 3g and h), but significantly reduced blastocyst formation rate (Day 7) compared to the control groups (Fig. 3g and i) ($P < 0.05$). In addition, *METTL3* OE resulted in a significant reduction in the number of total cells, ICM cells, and TE cells (Fig. 3j and k) ($P < 0.05$). However, the ratio of ICM cells to TE cells in the *METTL3* OE blastocysts did not change compared to the control groups (Fig. 3k). Altogether, these results demonstrate that overexpression of *METTL3* impaired blastocyst development and normal lineage allocation.

METTL3 negatively regulates autophagy activity of early embryos in an m6A-dependent manner

METTL3 was recently reported to negatively regulate autophagy in cardiomyocytes [26], which prompted us to investigate whether METTL3 regulates embryo development via autophagy. Morula was then subjected to qPCR analysis to examine the relative expression of several key genes involved in autophagy and apoptosis. *METTL3* KD caused a significant increase in expression of *ATG5*, *BECLIN1*, and *CASPASE3* (Fig. 4a) ($P < 0.05$), whereas *METTL3* OE induced decrease of *ATG5* expression (Fig. 4b) ($P < 0.05$), This suggested a potential involvement of METTL3 in controlling *AGT5* expression in porcine embryos. To verify the effect of METTL3 on ATG5 protein expression, we detected the ATG5 by immunofluorescence staining. The specificity of the commercially available ATG5 antibody was first confirmed in porcine embryos (additional file 1c). Immunofluorescence staining showed that *METTL3* KD significantly increased ATG5 protein levels (Fig. 4c) ($P < 0.05$) whereas *METTL3* OE decreased ATG5 protein levels in morula (Fig. 4d) ($P < 0.05$). In addition, TUNEL staining revealed that *METTL3* KD did not increase apoptotic cell number (additional file 3a and b), but caused a significant increase in apoptosis ratio of the resulting blastocysts (additional file 3c) ($P < 0.05$).

Given that ATG5 acts as an upstream core regulator of autophagy pathway, we speculated that METTL3 might affect autophagy activity through regulating ATG5 expression. To address this, protein levels of LC3 (Light chain 3), an autophagy marker, were measured by immunofluorescence to determine autophagy activation in embryos. The specificity of LC3 antibody was validated in preliminary experiments (additional file 1d). Of note, *METTL3* KD or OE led to a significant increase in protein levels of LC3 at the morula stage compared to the control groups, suggesting an elevation of autophagy activity (Fig. 4e and f) ($P < 0.05$). Taken together, these data support that *METTL3* KD or OE impaired the ATG5 expression and enhanced the autophagy activity in porcine embryos.

In the next set of experiments we examined whether *METTL3* regulates ATG5 expression via m6A modification of *ATG5* mRNAs. A web-based application tool called SRAMP was used to predict m6A sites in *ATG5* mRNA. As shown in Fig. 4g, m6A modifications are primarily present at 3'UTR of *ATG5* mRNA. To examine whether METTL3-mediated m6A modification regulated *ATG5* expression through modulating mRNA decay, we conducted the analysis of *ATG5* mRNA stability in embryos. The results revealed that *METTL3* KD enhanced stability of the preexisting *ATG5* mRNA compared to the control group (Fig. 4h) ($P < 0.05$), suggesting that METTL3 regulates ATG5 expression via mediating its mRNA stability. Collectively, these data indicate that METTL3 negatively regulating autophagy activity of early embryos depends on decay of m6A-modified *ATG5* mRNA.

METTL3-mediated m6A methylation exerts inhibitory effects on autophagy activity in the trophectoderm lineage

It was reported that autophagy was preferentially restricted to the TE lineage in mouse blastocysts [13] and METTL3 specifically regulated TE cell proliferation in porcine blastocysts. Thus, we hypothesized that METTL3 might exert TE lineage-specific inhibitory effects on autophagy activity in porcine blastocysts. To test this hypothesis, immunofluorescence was performed to examine the localization and levels of m6A and LC3 in the ICM and TE lineages. The results showed that *METTL3* KD reduced m6A

levels in both ICM and TE lineages (Fig. 5a). LC3 levels appeared to be only decreased in the TE lineage of *METTL3* KD blastocysts whereas it seemed to be not changed in the ICM lineage between the control and *METTL3* KD groups (Fig. 5b), suggesting a preferential role of METTL3 in autophagy in the TE lineage. To further confirm the differential effects of METTL3 on autophagy activity between ICM and TE lineages, blastocysts in each group were separated into individual blastomeres (Fig. 5c), which in turn were subjected to quantitative analyses of *SOX2* and *CDX2* mRNA to identify the ICM and TE cells (Fig. 5d). Meanwhile, single cell qPCR revealed that *METTL3* KD resulted in a significant increase in expression levels of *ATG5* and *BECLIN1* in the TE cells (Fig. 5e) ($P < 0.05$), but did not affect expression of the two genes in the ICM cells (Fig. 5f). Interestingly, *METTL3* KD led to a significant reduction in expression levels of *BECLIN1* in the ICM cells (Fig. 5f) ($P < 0.05$). Together, these date imply that METTL3-mediated m6A methylation preferentially inhibits autophagy activity in the trophectoderm lineage.

Autophagy inhibitor partially rescues development and quality of *METTL3* knockdown embryos

To clarify if autophagy mediates the effect of *METTL3* on embryo development, we reduced autophagy level by autophagy inhibitor 3MA and examined if this could rescue the defects of embryo development. 3MA was added into culture medium. Untreated and *METTL3* KD embryos served as the control groups. Immunofluorescence analyses showed that 3MA supplement reduced the autophagy in *METTL3* KD blastocysts to a level similar to that in the untreated control group (Fig. 6a and b) ($P < 0.05$). Of note, 3MA supplement partially rescued the defects of blastocyst formation by *METTL3* KD (Fig. 6c and d). Moreover, total cell number of blastocysts was significantly increased in 3MA treatment group compared to *METTL3* KD group (Fig. 6e) ($P < 0.05$). Therefore, these data indicate that restoration of autophagy levels partially rescued development and quality of *METTL3* KD embryos.

Discussion

A recent study reported an essential role of METTL3-mediated m6A methylation in blastocyst formation in mice [25], but its molecular mechanisms underlying blastocyst development are yet to be known. Our data in porcine embryos indicate that METTL3-mediated m6A methylation sustains blastocyst development via repressing autophagy activity. METTL3 negatively regulates expression of *ATG5* mRNA in the TE lineage in an m6A-dependent manner. Therefore, we propose a working model in which METTL3 supports blastocyst development through negatively regulating expression of m6A-modified *ATG5* mRNA that is required for autophagy activation (Fig. 7). To our knowledge, this work represents the first report characterizing the epitranscriptomic regulatory mechanism underlying mammalian blastocyst development.

The physiology levels of autophagy are indispensable for blastocyst development in mice [30] and pigs [11]. On the contrary, excessive levels of autophagy are detrimental to blastocyst development [31–33]. In this study, we showed that KD or enforced expression of *METTL3* severely impaired porcine blastocyst

development. In addition, *METTL3* loss or gain of function resulted in a significant increase or reduction in ATG5 expression and autophagy levels, respectively. It is thus possible that METTL3 mediated steady state of autophagy to allow blastocyst development in pigs. However, restoration of autophagy levels by the inhibitor treatment only partially rescued blastocyst development of *METTL3*-knockdown embryos, suggesting the existence of redundant mechanisms of METTL3 regulating blastocyst development. Interestingly, previous studies in mice showed that maternal ATG5 was required for development to 4-cell embryo stage [10] whereas zygotic ATG5 was dispensable for normal embryo development [34]. In pigs, *METTL3* overexpression dramatically decreased ATG5 expression and blastocyst rate, but did not affect development to 2-cell and morula stage. This discrepancy could be due to the diverse functions of ATG5 between different species.

Previous study in mice indicated that TE cells in blastocysts possessed a higher autophagy activity than ICM cells [13]. The high autophagy of TE cells met its requirement for much more energy [5]. Inhibition and induction of autophagy resulted in defects in the TE and ICM, and failure to separate the ICM and TE cells in mice [30]. Similarly, in pigs, repression of basal autophagy decreased total and TE cell number in blastocysts [33] and increased autophagy levels also disrupted proliferation and differentiation of TE cells [35]. Consistent with these studies, we found in this study that *MELLT3* KD or OE led to an increased or decreased autophagy, and caused fewer total cells and TE cells. Importantly, correction of autophagy levels could partially restore the total cell number in *METTL3* KD blastocysts. Therefore, we reasoned that abnormal autophagy levels at least partially accounted for TE lineage defects induced by METTL3 dysfunction in porcine blastocysts.

Recently, m6A modification was reported to inhibit autophagy activity in several cellular contexts [26–28]. In this study, we observed that the levels of *ATG5* mRNA were increased or decreased upon *METLL3* KD or OE. ATG5 binds to ATG12 and ATG16L to facilitate the conjugation of autophagy marker LC3 and autophagosome [36]. Thus, we identified a corresponding increase or decrease in the LC3 levels in *METLL3* KD or OE embryos. Studies indicated that m6A modification has been strongly linked to increased mRNA degradation [37]. Our data further showed that m6A modification mostly happened at 3'UTR of *ATG5* mRNA and m6A levels were increased or decreased upon *METTL3* KD or OE. Thus, these data demonstrate that METTL3 negatively regulates expression of *ATG5* mRNA in an m6A-dependent manner. Based on these analyses, METTL3 suppresses autophagy likely by destabilizing ATG5 at the transcript level.

Conclusions

Our findings show that METTL3-mediated m6A methylation negatively regulates autophagy to support blastocyst development in pigs. Our results may provide new insights into the function and potential mechanisms of METTL3 and m6A modification in regulating autophagy and mammalian blastocyst development.

Abbreviations

m6A, N^6-methyladenosine; METTL3, methyltransferase-like protein 3; METTL14, methyltransferase-like protein 14; WTAP, WT1 Associated Protein; FTO, fat mass and obesity-associated protein; ATG5, Autophagy related 5; LC3, light chain 3; ICM, inner cell mass; TE, trophectoderm; mTOR, mammalian target of rapamycin; qPCR, CDS, coding sequence; PA, parthenogenetic activation; IVF, *in vitro* fertilization; PCA, principal component analysis; SOX2, SRY-box transcription factor 2; CDX2, caudal type homeobox 2; OCT4, octamer-binding transcription factor 4; GV, germinal vesicle; MII, metaphase II.

Declarations

Funding

This work was supported by grants from the Anhui Provincial Natural Science Foundation (1908085MC97), the Open Fund of State Key Laboratory of Genetic Resources and Evolution (GREKF18-16), the Open Foundation of State Key Laboratory of Agrobiotechnology (2018SKLAB6-3), the National Natural Science Foundation of China (31802059 and 31902226), the Hefei Innovation and Entrepreneurship Support Plan for Returnee Scholar, and the Science and Technology Major Project of Anhui province (18030701185).

Acknowledgments

We thank MS. Xu Tong, Dandan Zhang and Mr. Shang Ren, Zhenyuan Ru, Tenglong Guo for their help in technical assistance.

Availability of data and materials

All data generated or analyzed during this study are included in this published article and its supplementary files.

Authors' contributions

ZC, JK, AS and YZ conceived the project and wrote the manuscript. ZH, RH, YW, XQ, WN, TX and DG performed the experiments. YM, TY and YL analyzed the data. All authors read and approved the final manuscript.

Ethics approval

All experiments were conducted according to the Institutional Animal Care and Use Committee (IACUC) guidelines under current approved protocols at Anhui Agricultural University.

Consent for publication

Not applicable.

Competing interest

The authors declare no conflicts of interest with regard to the study.

References

1. White MD, Plachta N. Specification of the First Mammalian Cell Lineages In Vivo and In Vitro. Cold Spring Harb Perspect Biol. 2020; 12.
2. Artus J, Hue I, Acloque H. Preimplantation development in ungulates: a 'menage a quatre' scenario. Reproduction. 2020; 159: 151-72.
3. Chazaud C, Yamanaka Y. Lineage specification in the mouse preimplantation embryo. Development. 2016; 143: 1063-74.
4. Kaneko KJ. Metabolism of Preimplantation Embryo Development: A Bystander or an Active Participant? Curr Top Dev Biol. 2016; 120: 259-310.
5. Houghton FD. Energy metabolism of the inner cell mass and trophectoderm of the mouse blastocyst. Differentiation. 2006; 74: 11-8.
6. Kumar RP, Ray S, Home P, Saha B, Bhattacharya B, Wilkins HM, et al. Regulation of energy metabolism during early mammalian development: TEAD4 controls mitochondrial transcription. Development. 2018; 145.
7. Wesselborg S, Stork B. Autophagy signal transduction by ATG proteins: from hierarchies to networks. Cell Mol Life Sci. 2015; 72: 4721-57.
8. Gao H, Khawar MB, Li W. Essential role of autophagy in resource allocation during sexual reproduction. Autophagy. 2020; 16: 18-27.
9. Liu Y, Levine B. Autosis and autophagic cell death: the dark side of autophagy. Cell Death Differ. 2015; 22: 367-76.
10. Tsukamoto S, Kuma A, Murakami M, Kishi C, Yamamoto A, Mizushima N. Autophagy is essential for preimplantation development of mouse embryos. Science. 2008; 321: 117-20.
11. Lee HR, Gupta MK, Kim DH, Hwang JH, Kwon B, Lee HT. Poly(ADP-ribosyl)ation is involved in pro-survival autophagy in porcine blastocysts. Mol Reprod Dev. 2016; 83: 37-49.
12. Xu YN, Shen XH, Lee SE, Kwon JS, Kim DJ, Heo YT, et al. Autophagy influences maternal mRNA degradation and apoptosis in porcine parthenotes developing in vitro. J Reprod Dev. 2012; 58: 576-84.
13. Lee JE, Oh HA, Song H, Jun JH, Roh CR, Xie H, et al. Autophagy regulates embryonic survival during delayed implantation. Endocrinology. 2011; 152: 2067-75.
14. Hu LF. Epigenetic Regulation of Autophagy. Adv Exp Med Biol. 2019; 1206: 221-36.
15. Nachtergaele S, He C. Chemical Modifications in the Life of an mRNA Transcript. Annu Rev Genet. 2018; 52: 349-72.
16. Shi H, Wei J, He C. Where, When, and How: Context-Dependent Functions of RNA Methylation Writers, Readers, and Erasers. Mol Cell. 2019; 74: 640-50.

17. Huang H, Weng H, Chen J. The Biogenesis and Precise Control of RNA m(6)A Methylation. Trends Genet. 2020; 36: 44-52.
18. Lin Z, Tong MH. m(6)A mRNA modification regulates mammalian spermatogenesis. Biochim Biophys Acta Gene Regul Mech. 2019; 1862: 403-11.
19. Xu K, Yang Y, Feng GH, Sun BF, Chen JQ, Li YF, et al. Mettl3-mediated m(6)A regulates spermatogonial differentiation and meiosis initiation. Cell Res. 2017; 27: 1100-14.
20. Sui X, Hu Y, Ren C, Cao Q, Zhou S, Cao Y, et al. METTL3-mediated m(6)A is required for murine oocyte maturation and maternal-to-zygotic transition. Cell Cycle. 2020; 19: 391-404.
21. Xia H, Zhong C, Wu X, Chen J, Tao B, Xia X, et al. Mettl3 Mutation Disrupts Gamete Maturation and Reduces Fertility in Zebrafish. Genetics. 2018; 208: 729-43.
22. Qi ST, Ma JY, Wang ZB, Guo L, Hou Y, Sun QY. N6-Methyladenosine Sequencing Highlights the Involvement of mRNA Methylation in Oocyte Meiotic Maturation and Embryo Development by Regulating Translation in Xenopus laevis. J Biol Chem. 2016; 291: 23020-26.
23. Wang YK, Yu XX, Liu YH, Li X, Liu XM, Wang PC, et al. Reduced nucleic acid methylation impairs meiotic maturation and developmental potency of pig oocytes. Theriogenology. 2018; 121: 160-67.
24. Zhao BS, Wang X, Beadell AV, Lu Z, Shi H, Kuuspalu A, et al. m(6)A-dependent maternal mRNA clearance facilitates zebrafish maternal-to-zygotic transition. Nature. 2017; 542: 475-78.
25. Kwon J, Jo YJ, Namgoong S, Kim NH. Functional roles of hnRNPA2/B1 regulated by METTL3 in mammalian embryonic development. Sci Rep. 2019; 9: 8640.
26. Song H, Feng X, Zhang H, Luo Y, Huang J, Lin M, et al. METTL3 and ALKBH5 oppositely regulate m(6)A modification of TFEB mRNA, which dictates the fate of hypoxia/reoxygenation-treated cardiomyocytes. Autophagy. 2019; 15: 1419-37.
27. Jin S, Zhang X, Miao Y, Liang P, Zhu K, She Y, et al. m(6)A RNA modification controls autophagy through upregulating ULK1 protein abundance. Cell Res. 2018; 28: 955-57.
28. Wang X, Wu R, Liu Y, Zhao Y, Bi Z, Yao Y, et al. m(6)A mRNA methylation controls autophagy and adipogenesis by targeting Atg5 and Atg7. Autophagy. 2019: 1-15.
29. Wei Q, Li R, Zhong L, Mu H, Zhang S, Yue L, et al. Lineage specification revealed by single-cell gene expression analysis in porcine preimplantation embryos. Biol Reprod. 2018; 99: 283-92.
30. Lee SE, Hwang KC, Sun SC, Xu YN, Kim NH. Modulation of autophagy influences development and apoptosis in mouse embryos developing in vitro. Mol Reprod Dev. 2011; 78: 498-509.
31. Kim MG, Kim DH, Lee HR, Lee JS, Jin SJ, Lee HT. Sirtuin inhibition leads to autophagy and apoptosis in porcine preimplantation blastocysts. Biochem Biophys Res Commun. 2017; 488: 603-08.
32. Song BS, Yoon SB, Kim JS, Sim BW, Kim YH, Cha JJ, et al. Induction of autophagy promotes preattachment development of bovine embryos by reducing endoplasmic reticulum stress. Biol Reprod. 2012; 87: 8, 1-11.
33. Song BS, Kim JS, Kim YH, Sim BW, Yoon SB, Cha JJ, et al. Induction of autophagy during in vitro maturation improves the nuclear and cytoplasmic maturation of porcine oocytes. Reprod Fertil Dev.

2014; 26: 974-81.
34. Kuma A, Hatano M, Matsui M, Yamamoto A, Nakaya H, Yoshimori T, et al. The role of autophagy during the early neonatal starvation period. Nature. 2004; 432: 1032-6.
35. Luo Z, Xu X, Sho T, Zhang J, Xu W, Yao J, et al. ROS-induced autophagy regulates porcine trophectoderm cell apoptosis, proliferation, and differentiation. Am J Physiol Cell Physiol. 2019; 316: C198-C209.
36. Guan JL, Simon AK, Prescott M, Menendez JA, Liu F, Wang F, et al. Autophagy in stem cells. Autophagy. 2013; 9: 830-49.
37. Lee Y, Choe J, Park OH, Kim YK. Molecular Mechanisms Driving mRNA Degradation by m(6)A Modification. Trends Genet. 2020; 36: 177-88.

Additional Files

Additional file 1: Verification of the specificity of primary antibodies. Antibodies including m6A (**a**), ATG5 (**c**) and LC3 (**d**) were tested on porcine 4-cell embryos and/or blastocysts. The primary antibody was replaced with blocking buffer to serve as a negative control. Representative images obtained by confocal microscopy are shown. Scale bar: 50 μm. (**b**) m6A antibody was tested on porcine 4-cell embryos before and after RNase A treatment. There were no any fluorescence signals in RNase A-treated embryos. Representative images obtained by confocal microscopy are shown. Scale bar: 50 μm.

Additional file 2: Effect of *METTL3* knockdown on development of early cleavage-stage embryos. The number of 2-cell, 4-cell, 8-cell and morula embryos was recorded and the developmental rate of embryos at each stage was statistically analyzed. All experiment was repeated three times. Data are shown as mean ± S.E.M.

Additional file 3: Effect of *METTL3* knockdown on apoptosis of blastocyst. (**a**) TUNEL staining in blastocysts. Red spots indicate apoptotic cells, blue spots mark nuclei. Representative images obtained by confocal microscopy are shown. Scale bar: 50 μm. (**b**) Analyses of apoptotic cell number in blastocysts. (**c**) Analyses of apoptosis ratio in blastocysts. All data are shown as mean ± S.E.M and different letters on the bars indicate significant differences ($P < 0.05$).

Figures

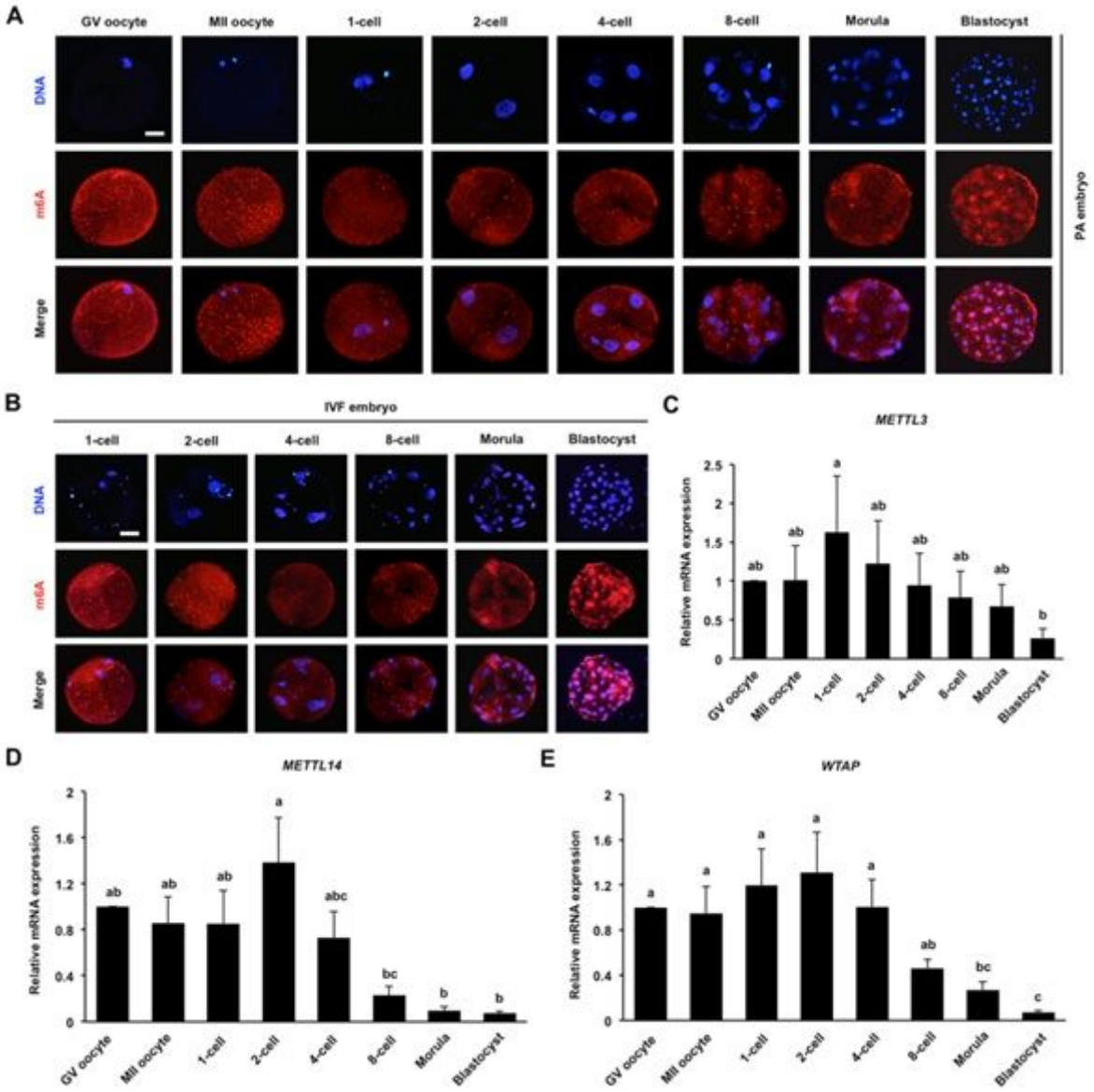

Figure 1

m6A methylation and its writers exist in early embryos (a, b) Levels and localization of m6A modification in PA and IVF embryos at different developmental stages. Embryos were stained to indicate m6A (red) and DNA (blue). Shown are representative images obtained by confocal microscopy. The experiment was independently repeated three times with at least 30 oocytes/embryos per stage. GV, germinal vesicle; MII, metaphase II. Scale bar: 50 μm. Expression of METTL3 (c), METTL14 (d) and WTAP (e) mRNA in oocytes and early embryos. The relative abundance of METTLE3, METTL14 and WTAP mRNA was determined by qPCR. Data were normalized against endogenous reference gene EF1α1 and the data from each stage were relative to GV oocyte. Data are shown as mean ± S.E.M and different letters on the bars indicate significant differences ($P < 0.05$).

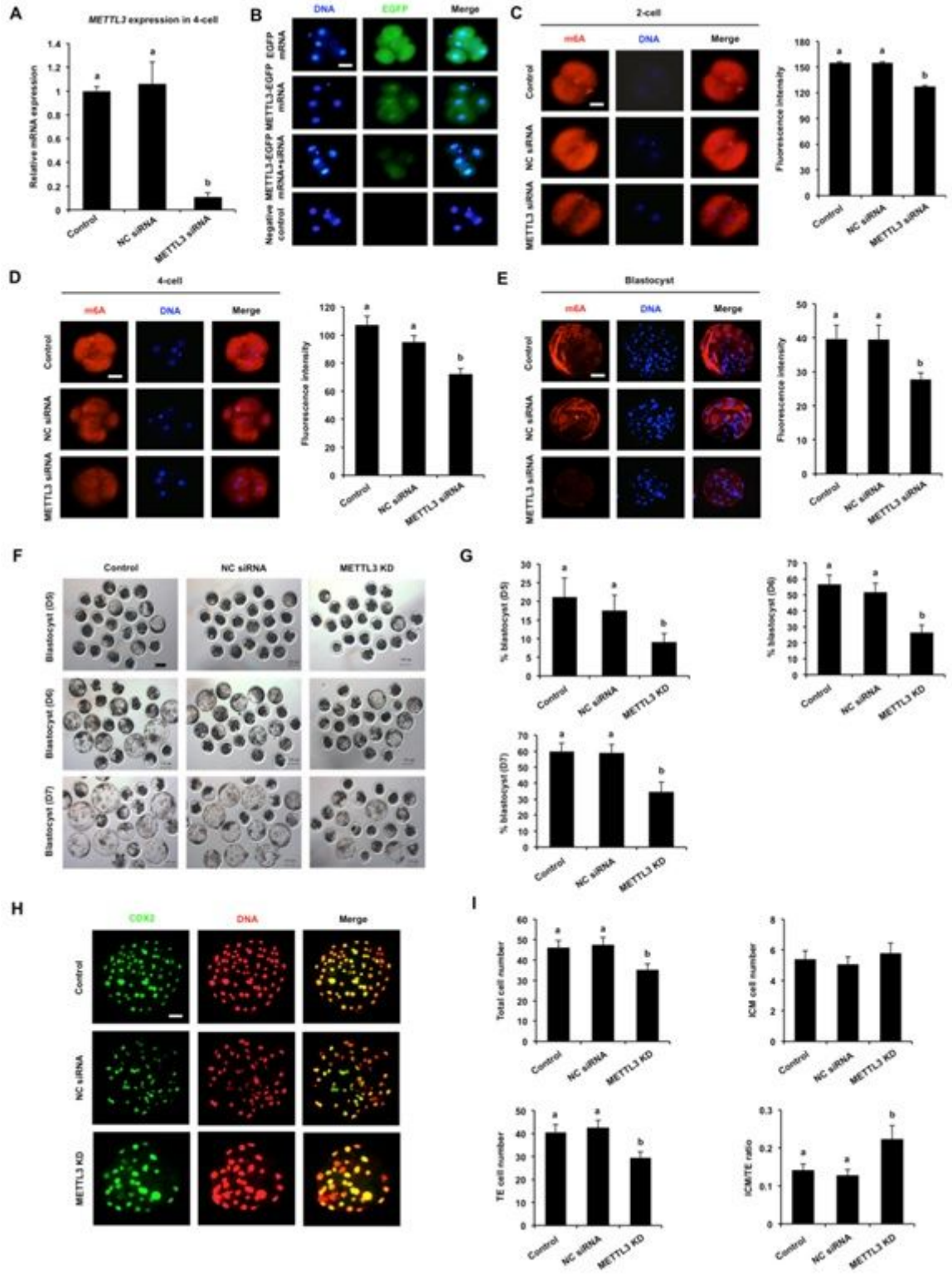

Figure 2

Effect of METTL3 knockdown on blastocyst development and lineage allocation (a) Expression levels of METTL3 mRNA in embryos. The relative abundance of METTL3 mRNA in 4-cell embryos from control, NC siRNA injection, and METTL3 siRNA (called as METTL3 knockdown or METTL3 KD) injection was determined by qPCR. NC, negative control. (b) Expression of METTL3 protein in 4-cell embryos. Embryos from the indicated groups were imaged for EGFP (green) and DNA (blue) by confocal microscopy and the

representative images are shown. The experiment was independently repeated three times with at least 30 embryos per stage. Scale bar: 50 μm. (c, d, e) Levels of m6A modification in embryos. Embryos from each group at 2-cell, 4-cell and blastocyst stage were stained for m6A (red) and DNA (blue). The fluorescence intensity was quantitatively analyzed by image J. Representative images obtained by confocal microscopy are shown. The experiment was independently repeated three times with at least 30 embryos per stage. Scale bar: 50 μm. (f) Representative images of blastocysts at different stages. Scale bar: 100 μm. (g) Developmental rates of porcine blastocysts. The rates of blastocysts at day 5, 6, and 7 were recorded and statistically analyzed in each group. (h) Immunofluorescence staining of blastocysts. Blastocysts were stained for CDX2 (green) and DNA (red). Representative images obtained using confocal microscopy are shown. The experiment was independently repeated three times with at least 15 blastocysts per group. Scale bar: 50 μm. (i) Lineage allocation analysis of METTL3 KD and control blastocysts. Total cell numbers, ICM cells, TE cells, and the ratio of ICM cells to TE cells were separately recorded and subjected to statistical analysis. ICM: inner cell mass; TE: trophectoderm. All data are represented as mean ± S.E.M and different letters on the bars indicate significant differences ($P < 0.05$).

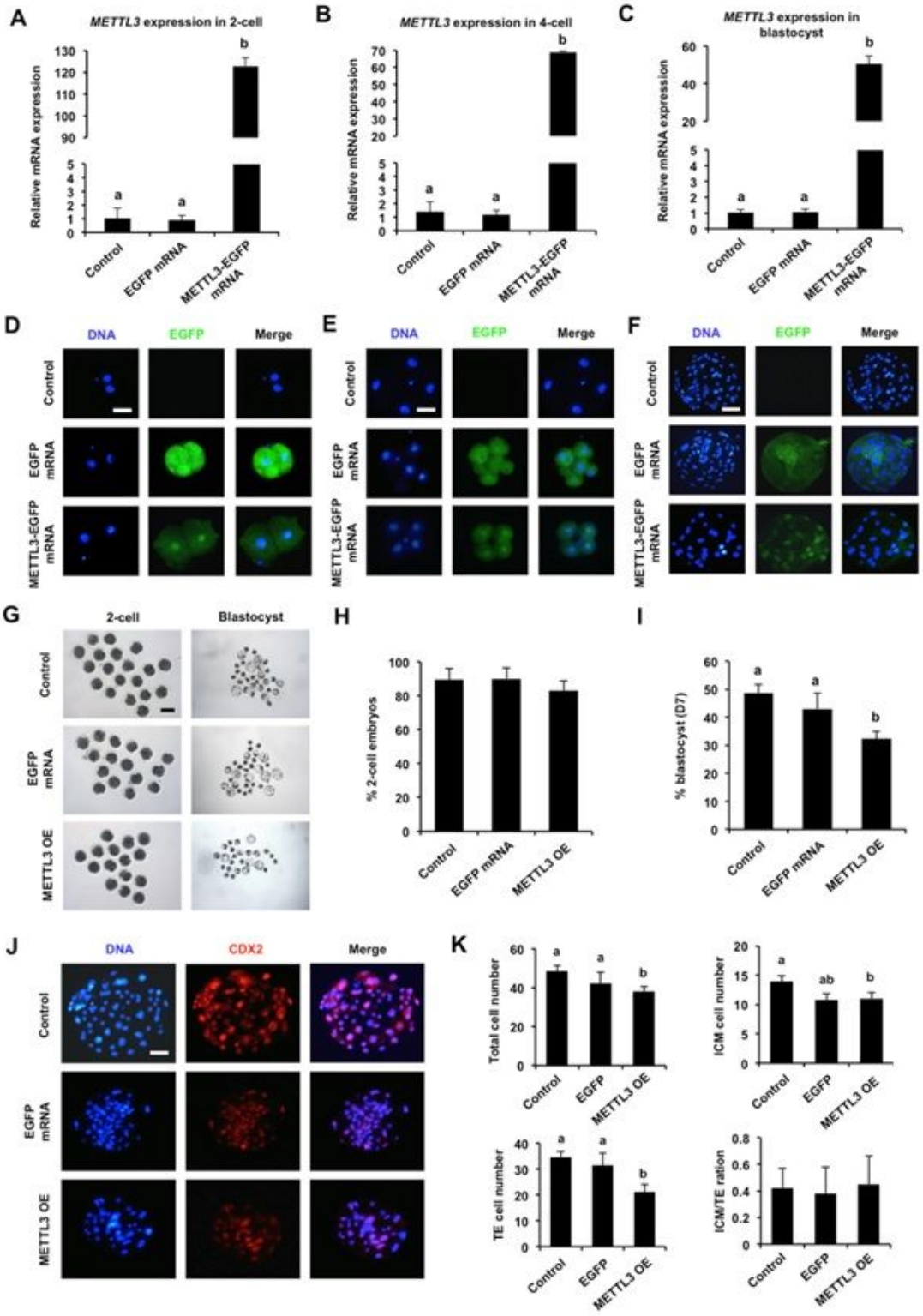

Figure 3

Effect of METTL3 overexpression on blastocyst development and lineage allocation (a, b, c) Expression levels of METTL3 mRNA in embryos. MII oocytes were microinjected with METTL3-EGFP mRNA (called as METTL3 overexpression or METTL3 OE). Uninjected oocytes or EGFP mRNA injected served as two control groups. The relative abundance of METTL3 mRNA in 2-cell, 4-cell and blastocysts was determined by qPCR. (d, e, f) Expression of METTL3 protein in embryos. Embryos at 2-cell, 4-cell and blastocyst stage

from each group were imaged for EGFP (green) and DNA (blue) by confocal microscopy and the representative images are shown. The experiment was independently repeated three times with at least 30 embryos per stage. Scale bar: 50 μm. (g) Representative images of blastocysts from each group. Scale bar: 100 μm. (h, i) Developmental rates of 2-cell embryos and blastocysts. (j) Representative fluorescence images of blastocysts. Blastocysts were stained for CDX2 (green) and DNA (red), and were imaged using confocal microscopy. The experiment was independently repeated three times with at least 15 blastocysts per group. Scale bar: 50 μm. (k) Lineage allocation analysis of METTL3 overexpression and control blastocysts. Total cell numbers, ICM cells, TE cells, and the ratio of ICM cells to TE cells were separately recorded and subjected to statistical analysis. ICM, inner cell mass; TE, trophectoderm. All data are represented as mean ± S.E.M and different letters on the bars indicate significant differences ($P < 0.05$).

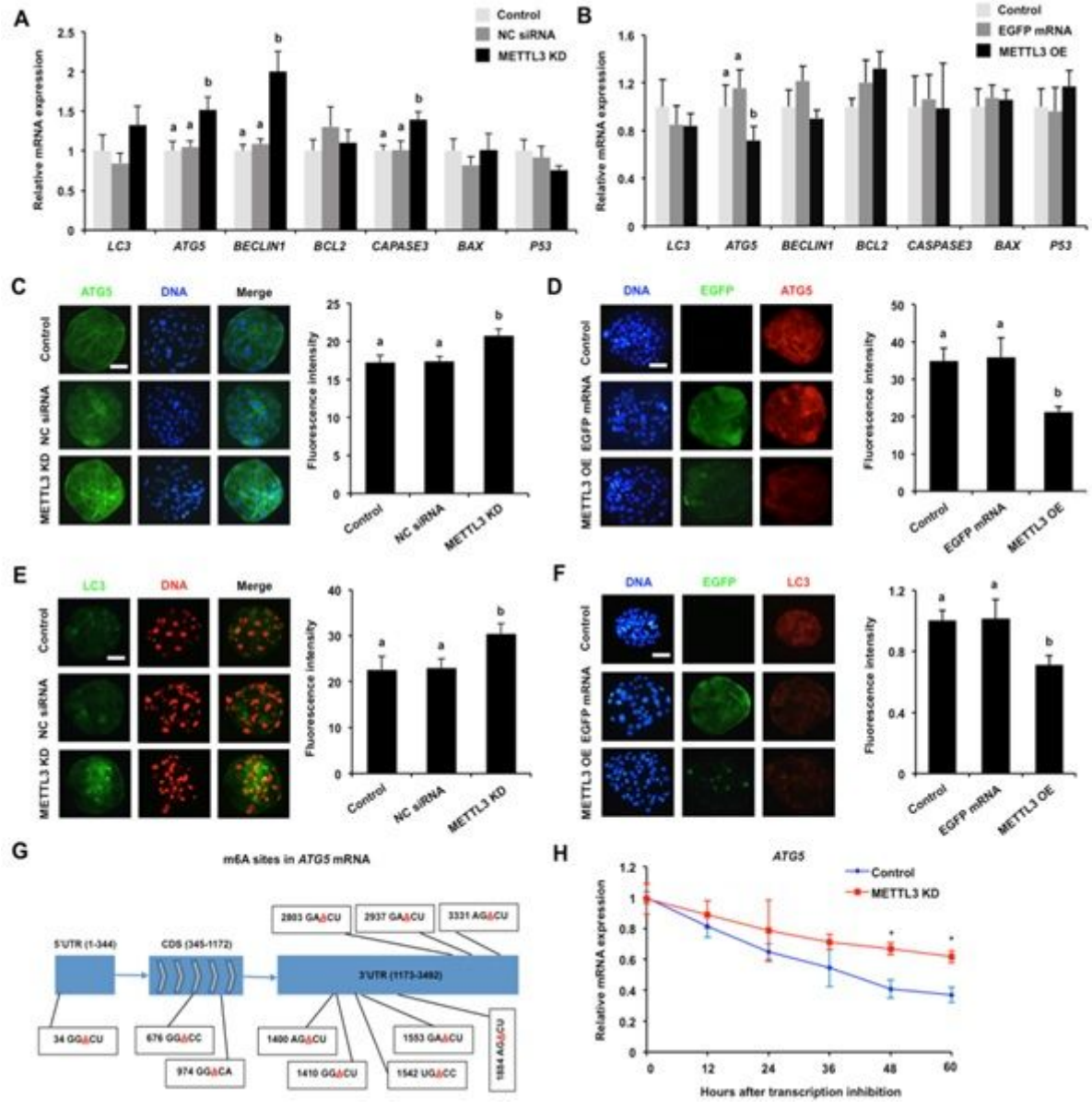

Figure 4

Effects of METTL3 loss or gain of function on autophagy activity in blastocysts (a, b) Expression levels of genes associated with autophagy and apoptosis in blastocysts. The relative expression of the indicated genes from control, NC siRNA or EGFP mRNA injection, and METTL3 KD or METTL3 OE was determined by qPCR. (c, d) Expression of ATG5 protein in blastocysts. Blatocysts from each group were stained for ATG5 and DNA. The fluorescence intensity was quantitatively analyzed by image J (right panel). Shown are representative images obtained by confocal microscopy. The experiment was independently repeated three times with at least 20 blastocysts per group. Scale bar: 50 μm. (e) Prediction of m6A methylation sites in ATG5 mRNA. m6A methylation sites in full-length sequence of ATG5 mRNA was predicted using a web tool (called as SRAMP) (f) Lifetime of ATG5 mRNA in control and MEKKL3 KD embryos. The relative abundance of ATG5 mRNA was determined by qPCR. Asterisks indicate significant differences ($p < 0.05$). (h, i) Expression of LC3 protein in blastocysts. Blatocysts from the indicated groups were stained for LC3 and DNA. The fluorescence intensity was quantitatively analyzed by image J (right panel). The experiment was independently repeated three times with at least 20 blastocysts per group. Scale bar: 50 μm. All data are shown as mean ± S.E.M and different letters on the bars indicate significant differences ($P < 0.05$).

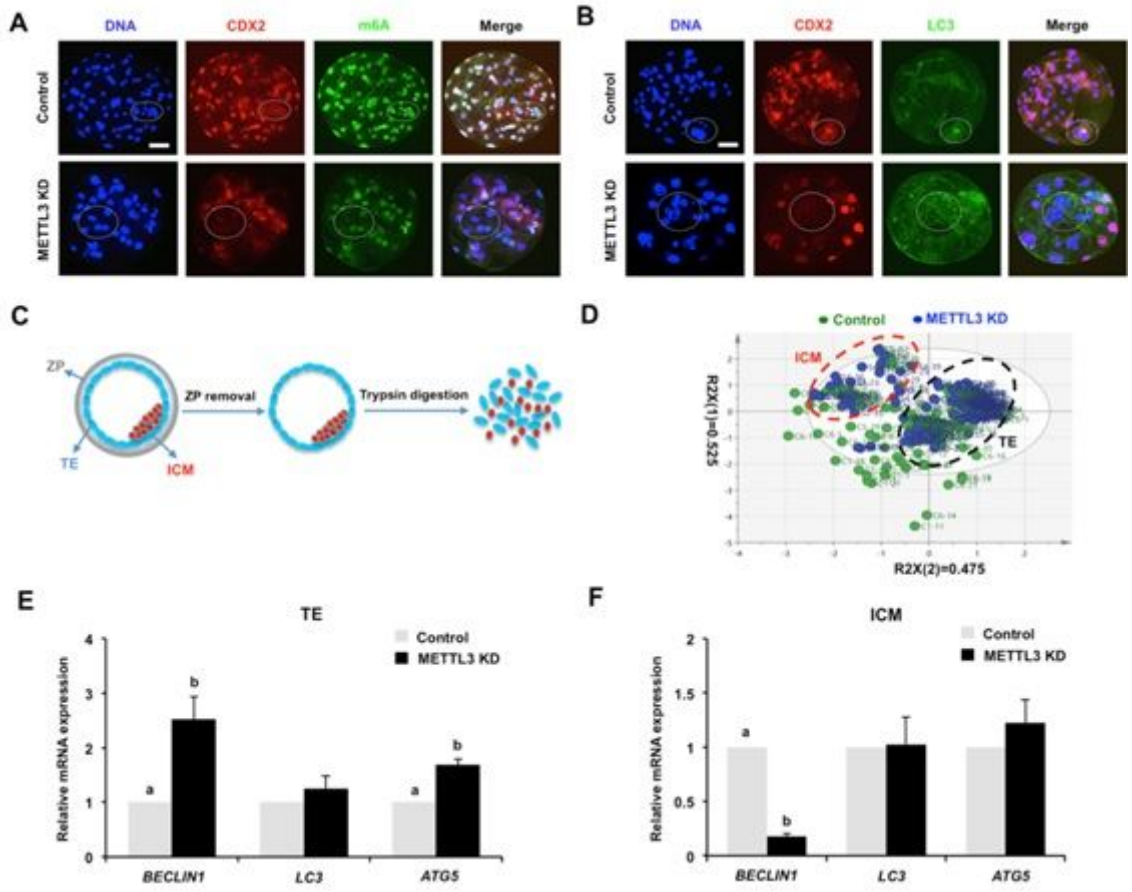

Figure 5

Differential effects of METTL3 knockdown on autophagy activity between TE and ICM lineage (a) Levels of m6A modification in the control and METTL3 KD blastocysts. Blastocysts were stained for CDX2 (red), m6A (green) and DNA (blue). (b) Levels of LC3 protein in control and METTL3 KD blastocysts.

Blastocysts were stained for CDX2 (red), LC3 (green) and DNA (blue). The experiment was independently repeated three times with at least 20 blastocysts per group. White dashed circles in A and B indicate inner cell mass. Scale bar: 50 μm. (c) Schematic diagram of separation of single blastomere from blastocysts. ZP: zonal pellucida; ICM: inner cell mass; TE: trophectoderm. (d) Identification of ICM and TE cells in the control and METTL3 KD blastocysts. The expression of SOX2 and CDX2 mRNA for each blastomere was quantified by single-cell qPCR. Cell identity is then clustered by principal component analysis (PCA). Red dashed circles indicate inner cell mass (ICM), black dashed circles denote trophectoderm (TE). Expression of genes related with autophagy in TE (e) and ICM (f) cells. The expression of the indicated genes in TE or ICM was quantified by single-cell qPCR. All data are shown as mean ± S.E.M and different letters on the bars indicate significant differences ($P < 0.05$).

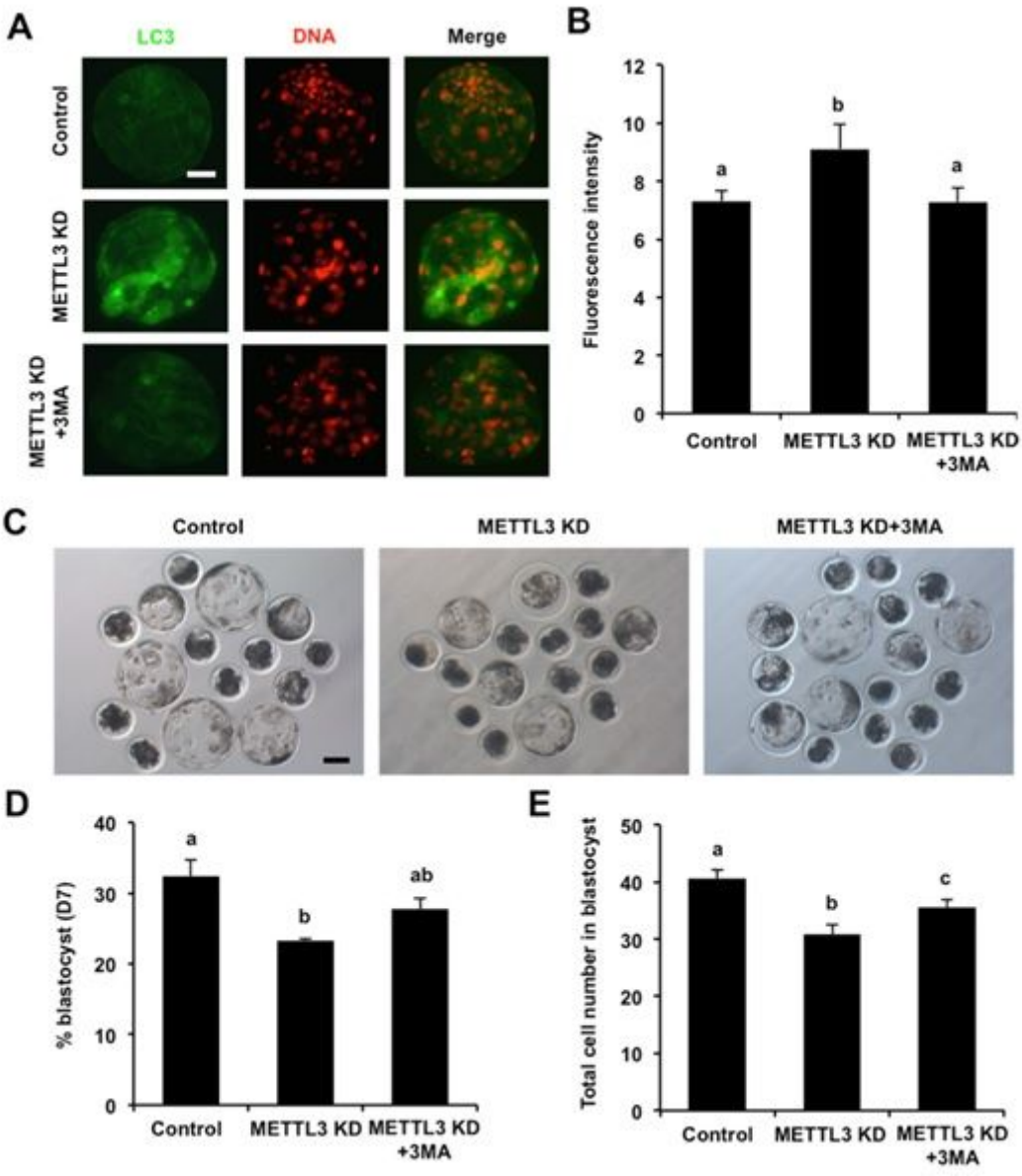

Figure 6

Effect of autophagy inhibitor supplementation on development and quality of METTL3 knockdown embryos (a) Levels of LC3 protein in blastocysts. Blastocysts from control, METTL3 KD and METTL3 KD

plus 3MA (autophagy inhibitor) were stained for LC3 (green) and DNA (red). The fluorescence intensity was quantitatively analyzed by image J (b). The experiment was independently repeated three times with at least 20 blastocysts per group. Scale bar: 50 μm. (c) Representative images of blastocysts at day 7. METTL3 KD embryos were cultured in medium supplemented with 3MA. Untreated or METTL3 KD embryos served as two control groups. Scale bar: 100 μm. (d) Developmental rates of porcine blastocysts. The rates of blastocysts at day 7 were recorded and statistically analyzed in each group. (e) Total cell number of blastocysts from each group. All data are shown as mean ± S.E.M and different letters on the bars indicate significant differences ($P < 0.05$).

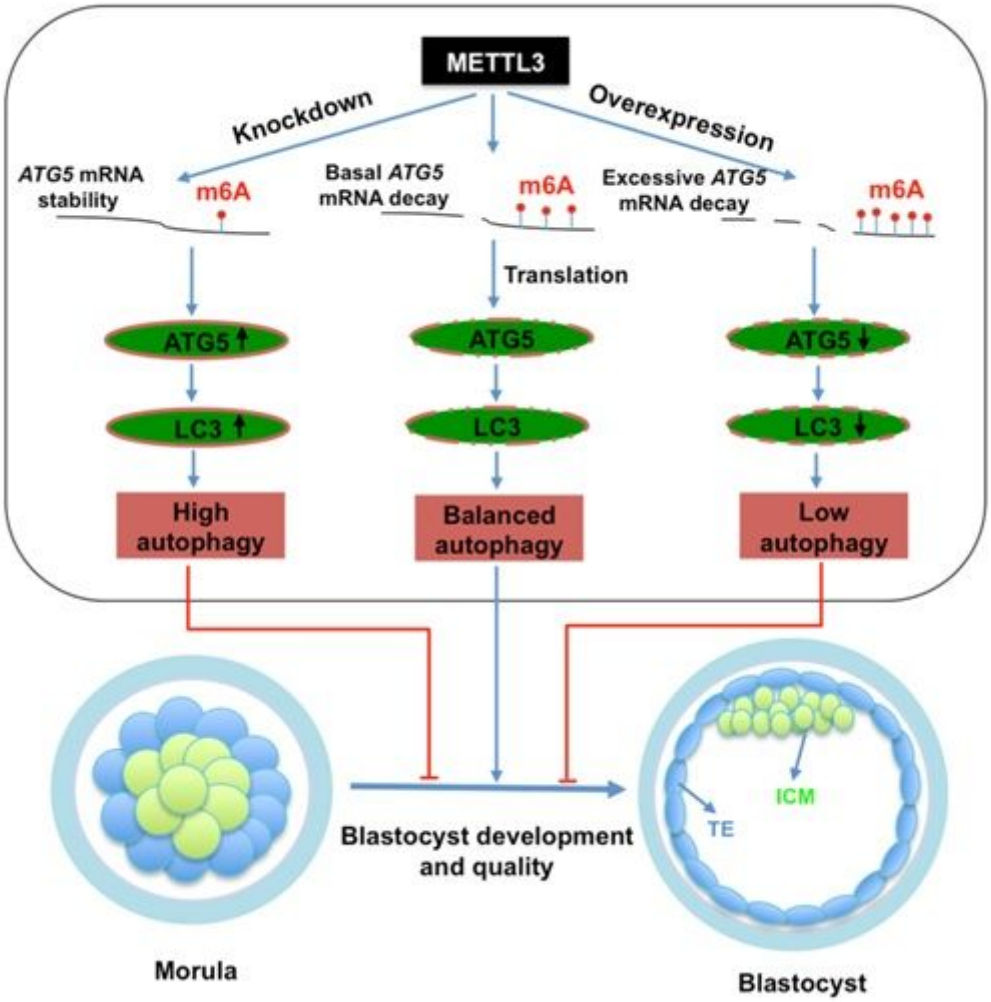

Figure 7

Working model illustrating how METTL3-mediated m6A methylation negatively regulates autophagy to support porcine blastocyst development In the normal TE cells, METTL3 generates proper m6A levels of ATG5 mRNA, thereby maintaining basal translation of ATG5 mRNA and normal ATG5 protein levels, sustaining appropriate expression of LC3 protein, physiological levels of autophagy and normal blastocyst development. On the contrary, METTL3 knockdown or overexpression separately caused inadequate or excessive m6A levels of ATG5 mRNA, leading to high or low translation of ATG5 mRNA, thereby resulting in high or low LC3 protein expression and autophagy levels and hindered the morula-to-

blastocyst transition. Collectively, METTL3-mediated m6A methylation negatively modulates autophagy in TE cells to sustain normal blastocyst development.

Supplementary Files

This is a list of supplementary files associated with this preprint. Click to download.

- Additionalfile2.pdf
- Additionalfile1.pdf
- Additionalfile3.pdf
- Additionalfile3.pdf
- Additionalfile2.pdf
- Additionalfile1.pdf